Nat Hazards
DOI 10.1007/s11069-017-3003-3

ORIGINAL PAPER

Spectral analysis of climate cycles to predict rainfall induced landslides in the western Mediterranean (Majorca, Spain)

Juan Antonio Luque-Espinar[1] · **Rosa María Mateos**[1] · **Inmaculada García-Moreno**[2] · **Eulogio Pardo-Igúzquiza**[2] · **Gerardo Herrera**[2]

Received: 11 November 2016 / Accepted: 19 July 2017

Abstract In the present work, spectral analysis has been applied to determine the presence and statistical significance of climate cycles in long-term data series from different rainfall and gauging stations located in the Tramuntana Range, in the north-western sector of the island of Majorca. Climate signals recorded previously in the Mediterranean region have been identified: the ENSO, NAO, HALE, QBO and Sun Spot cycles as well as others related to solar activity; the most powerful signals correspond to the annual cycle, followed by the 6-month and NAO cycles. The incorporation of data derived from gauging stations contributes to better climate signal detection as local and exceptional influences are eliminated. Simulations have been performed for each rainfall/gauging station, using the most significant climate cycles obtained by means of the power spectrum. A good correlation between rainfall/flow values and simulated cycles has been obtained. The NAO and ENSO cycles are the most influential in the rainy periods, and specifically the NAO cycle, where a good correlation between episodes of high rainfall/flow and high values of ANAOI can be observed. At a second stage, landslides dated and recorded in the Tramuntana Range since 1954 (174 events) have been correlated with the simulated cycles obtaining good results, as the landslide events match rainfall peaks well. The correlation for the past decade (since 2005), when a detailed landslide inventory is available, also

✉ Juan Antonio Luque-Espinar
ja.luque@igme.es

Rosa María Mateos
rm.mateos@igme.es

Inmaculada García-Moreno
inmaculada.garcia@igme.es

Eulogio Pardo-Igúzquiza
e.pardo@igme.es

Gerardo Herrera
g.herrera@igme.es

[1] Geological Survey of Spain (IGME), Regional Office in Granada, Urb. Alcázar del Genil. Edf. Zulema, bajos, 18006 Granada, Spain

[2] Geological Survey of Spain, Ríos Rosas, 23, 28003 Madrid, Spain

reveals a coincidence between landslide events and climate cycles, and specifically NAO and ENSO cycles. That is the case of the period 2008–2010, when numerous mass movements took place, and when the largest movement of the inventory was recorded. Results show a potential rainy period in the Tramuntana Range for the coming years (with maximum values around year 2021), when conditions similar to those related to the 2008–2010 event could take place again. The methodology presented in this work can contribute to the prediction of temporal, extreme hydrological events in order to design short-/medium-term mitigation strategies on a regional scale.

Keywords Climate cycles · Landslides · Mediterranean region · Prediction · Spectral analysis

1 Introduction

Natural hazards triggered exclusively by extreme hydrological events, known as water hazards, are usually periodic in occurrence (Saaroni et al. 2012). The primary forces driving this kind of natural disaster in many parts of the world have been natural climate cycles, especially El Niño (ENSO) and La Niña. Scientists have learned a great deal during the past few decades about how this strange "seesaw" in the equatorial Pacific affects weather worldwide. Extreme phases of the ENSO have also been found to have significant influence on both wet and drought conditions in the Mediterranean region (Muñoz-Díaz and Rodrigo 2005; Tramblay et al. 2013), and changes in Mediterranean precipitation are, in large part, associated with the variability of the North Atlantic Oscillation (NAO) (Xoplaki et al. 2012). In southern Europe, and specifically in the Mediterranean region, these and other natural cycles related to solar activity or global atmospheric dynamics can influence the climate pattern (Rodó et al. 1997). They can be summarised as follows:

- Cycles between 2 and 2.9 years, associated with the Quasi-Biennial Oscillation (QBO) (Labitzke and van Loon 1990).
- Cycles between 5 and 6 years may be a harmonic component of the 11-year sunspot cycle (Lamb 1977) or may be related to the *El Niño* Southern Oscillation (ENSO) (Stuiver and Braziunas 1989). Fleming and Quilty (2006) specify that the warm phase of the ENSO may range between 2 and 7 years.
- Cycles between 6 and 10 years which are identified with the NAO (Hurrell 1995; Pozo-Vázquez et al. 2000).
- Cycles between 10.5 and 12 years which represent the 11-year sunspot cycle (Stuiver and Braziunas 1989).
- Cycles between 20 and 25 years are associated with the Hale cycle (Hoyt and Schatten 1997).
- Those related to solar activity and lunar tidal cycles. Cycles of 18.6, 26.8 and 47.6 years have been reported (Currie et al. 1993; Pardo-Igúzquiza et al. 1994; Williams 1981).

Spectral analysis is a powerful statistical technique for analysing the distribution (over frequency) of the power contained in a signal, based on a finite set of data. It is very common for information to be encoded in the sinusoids that form a signal. This technique is widely used to identify patterns in long-term data series (Jenkins and Watts 1968; Pardo-Igúzquiza and Rodríguez-Tovar 2012), and more specifically, spectral analysis has been

applied to determine the presence and statistical significance of natural climate cycles in long-term series by processing data derived from meteorological stations (Knippertz 2003; Karagiannidis et al. 2007). Integrating data derived from aquifers, natural springs and gauging stations can support and substantially improve the statistical analysis as an inherent data screen is applied and the recorded signals are more significant (Luque-Espinar et al. 2008).

Different methods can be used to infer the power spectrum. Luque-Espinar et al. (2008) applied and compared some approaches from the literature: (1) the periodogram (Papoulis 1984), (2) the Blackman–Tukey approach (Blackman and Tukey 1958), (3) maximum entropy (Burg 1972) and (4) the Thomson multitaper method (Thomson 1982). They concluded that the Blackman–Tukey approach offers better results as the climate cycles are well identified and the statistical confidence is higher. This conclusion is also supported by Pardo-Igúzquiza and Rodríguez-Tovar (2012). Based on this, we have applied the Blackman–Tukey approach considering it to be the most adequate for this kind of analysis.

Within hydrological natural hazards, landslides are closely related to heavy rainfall events and there is a strong association between major landslide events (with numerous cases in the same region) and periods of extreme rainfall. In the last hundred years, several extreme climatic episodes have been identified as producing widespread landslide activity in Spain. The most significant took place in the Pyrenees in 1937, 1940 and 1982; in the Cantabrian range in 1983, and in the Baetic ranges in the winter of 1996–1997, all of them were related to unusual and abundant precipitations (Corominas 2006). Finally, another abnormal situation took place in Majorca (Balearic Islands) for the period spanning from 2008 to 2010, when a combination of persistent and intense precipitations caused a large number of slope failures (Mateos et al. 2012).

There is a vast literature correlating rainfall and landslide occurrence, which tries to determine the rainfall-triggering thresholds (e.g. Capparelli and Versace 2011; Guzzetti et al. 2008; Huang et al. 2015; Mathew et al. 2014; Piciullo et al. 2016; Staley et al. 2013; Terlien 1998; Wieczoreck 1996), and also several works that analyse the impact of climate and its changes on landslides (e.g. Coe and Godt 2012; Crozier 2010; Gariano and Guzzetti 2016). Although spectral analysis is a well-known technique in hydrological studies, there is a lack of previous work applying spectral analysis to correlate the occurrence of rainfall-induced landslides and natural climate cycles.

In the present paper, we have primarily carried out a spectral analysis of the integrated data from rainfall and gauging stations located throughout the Tramuntana Range (island of Majorca), in order to identify the natural climate cycles of relevance in this Mediterranean region. Additionally, the updated landslide inventory from the Geological Survey of Spain has been considered, selecting all, dated mass movements recorded in the Tramuntana Range since 1954 (174 events). During the second stage, numerous simulations have been performed to correlate the most significant climate cycles detected by means of spectral analysis (power spectrum) with the real rainfall/flow recorded. The best results have been compared with the temporal occurrence of landslides to determine the matching/mismatching of periods of heavy rain/flow and landslide events. The final stage is a short-term prediction of potential, significant landslide events in the region taking into account triggering climate conditions similar to those in the past.

The main objective of the present research is to show an application of spectral analysis, which can contribute to temporal regional landslide prediction in order to incorporate natural climate cycle knowledge into short-/medium-term mitigation strategies.

2 Test-site description

The island of Majorca, located in the western Mediterranean, has a variety of different geomorphological domains, most prominently the Tramuntana Range (1100 km^2) in the north-western part of the island (Fig. 1). The island has a typical Mediterranean climate, with mild winters and warm, dry summers. The maximum precipitation takes place during the autumn months (40% of total rainfall) when heavy storms are accompanied by intense rainfall with episodes of up to 300 mm in 24 h. The orography of the Tramuntana Range clearly controls the distribution of precipitation. The central sector (Lluc) registers average annual precipitation of 1500 mm, which gradually drops towards the SW extreme of the range (Calviá), where average annual precipitation is around 350 mm. The average

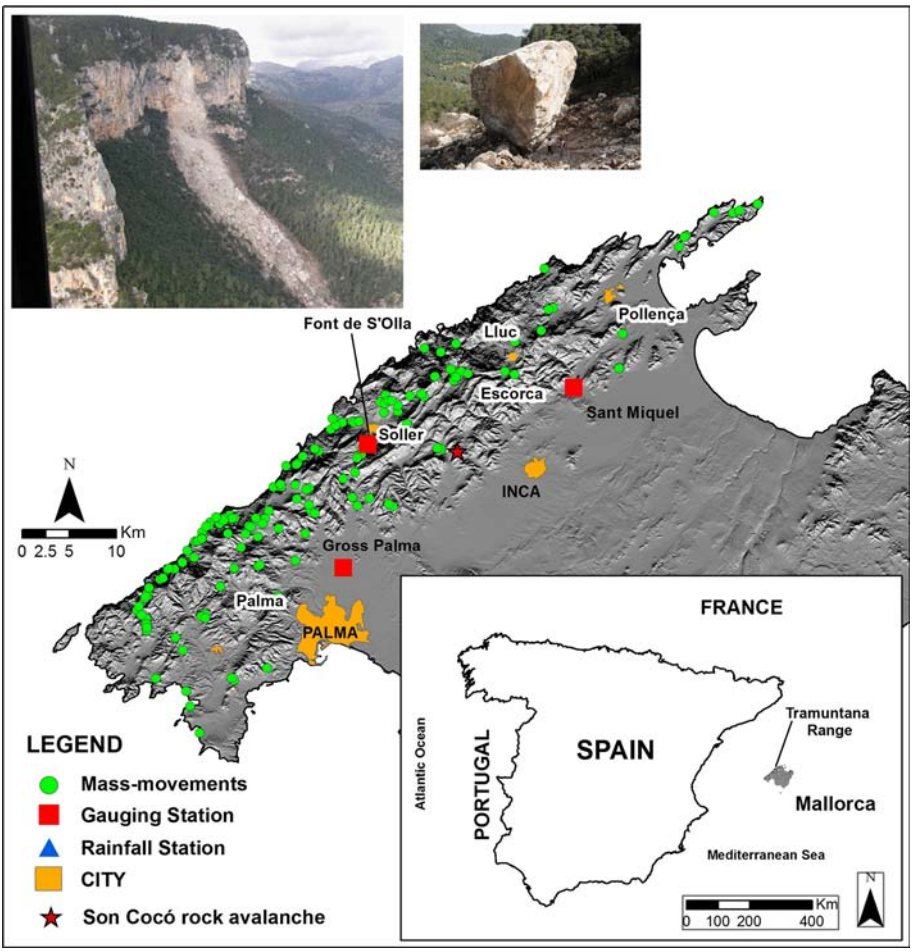

Fig. 1 Tramuntana range is located in the NW part of Majorca, in the western Mediterranean. Gauging and rainfall stations used for the present work have been represented as well as the location of the 174 landslides used in the present research. The Son Cocó rock avalanche can be considered the largest movement recorded since 1954; some photographs of Son Cocó are shown in the *upper part of the figure* as well as its location in the map

temperature is around 16 °C, with a maximum summer average of 30 °C and a minimum winter average of 7 °C. Nevertheless, it may freeze in winter and a few days of snow are usual in the range.

Owing to the torrential character of the rainfall and its marked seasonal nature, the water network on the island only has supply sporadically. There are no rivers on the island, only torrents, and thus, 90% of the island's water supply comes from aquifers. In the Tramuntana Range, short torrents with small drainage basins characterise the region. Taking into account the predominance of limestone lithologies, karstic aquifers and numerous water springs (around 700) characterise the hydrogeological behaviour of this region (Mateos et al. 2012).

The steep topography and geological complexity of the Tramuntana Range (numerous peaks with altitudes above 1000 m) influence intense slope dynamics with the consequent multiple types of slope failure (Mateos 2002; Mateos et al. 2007). The historical landslide inventory (almost 900 mass movement events reported since the eighteenth century) reveals that 70% of the events correspond to rockfalls because rocky, carbonated lithologies clearly predominate in the range (Mateos 2006; Mateos et al. 2015). Landslides and earth flows are also frequent phenomena affecting the soft sediments in the range, primarily clays and gypsum from the Late Triassic (Keuper). Most of the failures were reported after 1960 because there were few people living in the range before this time. In this sense, 183 mass movements from the inventory (including landslides and rockfalls) are correctly dated, and they are going to be used in the present work.

The relationship between extreme rainfall and reported landslides was analysed in previous studies in the Tramuntana region. Mateos et al. (2007) carried out a correlation of the known dates of historical landslides since 1956 with rainfall data provided by the rain gauges nearest to the location of the slides, revealing that most of the movements took place when maximum 24-h rainfall values are around 130 mm or above. The triggering threshold for rockfalls was considered to be 85 mm/day (Mateos 2006). There were no reliable data regarding rainfall accumulated during historical episodes due to incomplete records at the different weather stations in the range and the differing dates of installation.

The main criterion in selecting the Tramuntana Range for the present research was not only the existence of a detailed inventory, but also the recent occurrence of a significant event which caused numerous slope failures throughout the range. Between 2008 and 2010, the island of Majorca experienced the coldest and wettest winters of the last 40 years. The severe climate conditions triggered 66 mass movements in the range (Mateos et al. 2013). There is no evidence in the historical record (Mateos 2006) of any similar event, not only for the number of events but also for their magnitude.

Mateos et al. (2012) carried out a thorough analysis of the landslides/rockfalls triggered during this period and their relationship with meteorological data. As a general overview, they report for this period values of accumulated rainfall twice the average and values of daily rainfall up to 300 mm. On the 15 December 2008, a total of 296 mm of rain fell in 24 h near Sóller (Fig. 1), and the accumulated rainfall during hydrological year 2008–2009 was over 2260 mm, compared to the average annual precipitation of 1300 mm. Mateos et al. (2007) carried out a statistical analysis of intense rainfall in the Tramuntana range, using the Gumbel probability distribution function, which allowed us to obtain the maximum 24-h rainfall values for return periods of 5, 10, 25 and 100 years. The values obtained on the 15 December 2008 in the mountain range were very similar to those calculated for the return period of 100 years, which reflects the uniqueness of this extreme precipitation record.

3 Spectral analysis

3.1 Background

The statistical technique used to discover cyclic components in a time series is known as spectral analysis (Jenkins and Watts 1968; Yevjevich 1972; Bras and Rodríguez-Iturbe 1985). The signal component represents the structured part of the time series, made up of a small number of embedded periodicities or cycles repeated over a long time. The noise is a random component; it may be white noise, but more often will be red noise. A time series can be represented by a finite number of measurements. In the present case, a rainfall time series and gauging flow series are represented by a succession of measurements at regular or irregular time intervals. When one cyclic component contains any other cyclic component of a longer period than the length of the time series, it will give an apparent trend. This, together with possible real trends and other factors, gives rise to noise in the low frequencies, which is known as red noise.

Harmonic analysis is another name used to denote the estimation of cyclic components in the time series. The time series is supposed to be a linear combination of sinusoidal functions of known periods but of unknown amplitude and phase. The modulus of the amplitude is related to the variance of the time series, explained by the oscillation at each frequency. The representation of the square of the modulus versus frequency is known as the power spectrum. We have used the Blackman–Tukey (1958) indirect method because it is a robust approach which gives acceptable results with our datasets (Luque-Espinar et al. 2008).

The power spectrum (Pardo-Igúzquiza and Rodriguez-Tovar 2004) is calculated from the covariance function by:

$$\hat{S}(\omega) = \frac{1}{\pi}\left\{\lambda(0)\hat{C}(0) + \sum_{k=1}^{M}\lambda(k)\hat{C}(k)\cos(\omega k)\right\} \tag{1}$$

where $\hat{S}(\omega)$—estimated power spectrum for frequency ω; $\hat{C}(k)$—estimated covariance function for the kth lag; cos(·)—cosine; $\lambda(k)$—weighting function, known a lag window, which is used to give less weight to the covariance estimates as the lag increases. For large lags, the estimated covariance function is less reliable. The lag window used was the Tukey window:

$$\lambda(k) = \frac{1}{2}\left\{1 + \cos\left(\frac{\pi k}{M}\right)\right\} \quad 0 \le k \le M \tag{2}$$

M—maximum number of lags for the covariance function used in the spectral estimation. The maximum number of lags is $N - 1$, with N being the number of experimental data; however, with large values for M a great number of peaks will be seen in the estimated power spectrum, most representing spurious cycles. On the other hand, if M is very small, significant cycles will not be seen in the estimated power spectrum. For this reason, we used a value of $M = N/2$ in order to resolve peaks, and a value of $M = N/4$ to determine which peaks are the most significant.

In addition to using a small value for N, confidence levels were estimated for the inferred power spectrum. Our approach consists of fitting a background power spectrum with no cyclic component, but rather a smooth continuous spectrum, which is done by fitting the spectrum of an autoregressive process of order one, i.e. AR(1). The parameter of

this process is estimated from the experimental data. We then take into account the known result for the one-sided confidence band of the power spectrum estimator:

$$P\left(\upsilon\frac{\hat{S}(\omega)}{S(\omega)} < \chi^2_{\upsilon,\alpha}\right) = 1 - \alpha \tag{3}$$

where $P(\cdot)$—probability operator; $\hat{S}(\omega)$—power spectrum estimate for frequency ω; $S(\omega)$—underlying power spectrum for frequency ω; υ—number of degrees of freedom. For the Blackman–Tukey estimate with a Tukey lag window, the number of degrees of freedom is 2.67 N/M; $\chi^2_{\upsilon,\alpha}$—is the α quantile of a Chi-square distribution with υ degrees of freedom; α—significance level.

For this study, we established confidence levels (CL) of 90, 95 and 99%.

When cycles are well identified, simulations can be performed to reproduce their behaviour (Luque-Espinar et al. 2013). In this sense, calculating the amplitude and frequency for each cycle is necessary and is added to the most representative cycles.

3.2 Simulations

The simulations have been carried out by mean of frequency (F) and power spectrum (S). First, the amplitude is estimated for every cycle. In a general case, the next equation has been used:

$$P_i = \sigma^2 \frac{S_i}{(S_1 + \cdots + S_n)} \tag{4}$$

$$A_i = \sqrt{P_i} \tag{5}$$

A_i—cycle amplitude; last, a point is simulated by the next equation:

$$G_i = A_i \cos(2\pi t S_i + D) \tag{6}$$

G_i—simulated point for the time *t;* A_i—cycle amplitude *i; cos*—cosine; *t*—time; S_i—spectral value of the cycle; *D*—phase shift (radians). Change between 0 and 3.14 years; the simulated cycles have been fitted by a manual procedure.

3.3 Input data

3.3.1 Hydrological data

Only 3 of the 43 rainfall stations with monthly data record (AEMET, Spanish Meteorological Agency) distributed throughout the Tramuntana Range have ultimately been used for the present study (Table 1; Fig. 1), the main reason being the lack of data in most of the series. The most complete and constant rainfall station in the range is Pollença, located in the north-eastern sector of the range, in which a longer series (68 years) is available. Regarding gauging stations, only 3 of 39 have been used (Table 2; Fig. 1). The remaining 36 stations have been rejected because of the lack of data in the series, with no information for a long period of time and many zeros, which severely distorted the analysis. The selected gauging stations are: Gross Palma, Sant Miquel and Font de s´Olla. They are located at different altitudes in different sectors of the range (Fig. 1). The drainage basins have different surface areas, Gross Palma being the largest one (some 130 km^2). The Sant Miquel gauging station is located a few metres downstream of a group of natural and

Table 1 Statistical values from the rainfall stations used in the present research (STD: standard deviation)

Rainfall station	Data series	Mean (mm/month)	Median (mm/month)	STD (mm/month)	Min (mm/month)	Max (mm/month)	No. of data
Pollença	June 44–October 12	59.1	41.6	3774.9	0	385.6	769
Escorca	November 57–October 12	83.1	55.7	8022.3	0	714.8	768
Palma	January 78–December 12	36.9	27.8	1397.6	0	221.1	420

Table 2 Statistical values from the gauging stations used in the present research (STD: standard deviation)

Gauging station	Data series	Mean (m^3/month)	Median (m^3/month)	Var (m^3/month)	Min (m^3/month)	Max (m^3/month)	No. of data
Sant Miquel	January 68–September 09	1.6×10^6	0.15×10^6	8.5×10^6	0	17.1×10^6	501
Gross Palma	January 65–September 09	0.5×10^6	0×10^6	1.9×10^6	0	12.3×10^6	540
Font de S´Olla	January 76–December 09	0.3×10^6	0.13×10^6	0.2×10^6	0	4.0×10^6	405

intermittent springs called *Ses Fonts Ufanes de Gabellí*, with an annual average flow of 17×10^6 m^3 and peak flow rates of up to 70 m^3/s (Gelabert 2002). In this sense, the total data series obtained corresponds to the natural spring discharge in an area with scarce human pressure. The Font de S´Olla gauging station has similar conditions, as the station controls the discharge of a karstic spring located in a natural area with an annual average flow of 15×10^6 m^3 (Mateos and González 2009).

No gauges have been considered in the south-western part of the range, as no complete and continuous data are available.

3.3.2 Landslides

One hundred and seventy-four mass movements in the Tramuntana Range were used, all of which were taken from the inventory and are dated starting from 1954 (Table 3). For each landslide, day, month and year are known. One hundred and forty-one (81%) are rockfalls, with greatly varying volumes, ranging from 0.1 to 300,000 m^3. The remaining 33 events (19%) can be considered earth slides and their volumes range from 100 m^3 to 3×10^6 m^3. For both types of failure, frequency and volume have an inverse relationship. Table 3 also includes the information regarding the landslide volumes for each year, obtained adding up the volumes of the single landslides to show an approximate magnitude of the annual event. 2008 is the year with the highest landslide volume recorded. In December 2008, the Son Cocó rock avalanche took place in the central part of the range (Fig. 1). The rock avalanche destroyed the pine wood in its path, leaving a tongue of blocks over an area of 60,000 m^2, which was 300,000 m^3 in volume (Mateos et al. 2010). Son Cocó rock

Table 3 One hundred and seventy-four mass movements (rockfalls and earth slides) recorded in the Tramuntana Range since 1954 and used for the present work

Year	Number of events and failure type	Volume (m^3)	Year	Number of events and failure type	Volume (m^3)
1954	1 landslide	150×10^3	1999	1 landslide	
1973	1 landslide		2005	1 landslide 4 rockfalls	25×10^3
1974	1 landslide	20×10^3	2006	36 rockfalls	
1978	1 landslide		2007	4 landslides 13 rockfalls	
1983	1 landslide		2008	5 landslides 12 rockfalls	370×10^3
1987	1 landslide		2009	2 landslides 13 rockfalls	2×10^5
1993	2 landslides	100	2010	9 landslides 26 rockfalls	73×10^3
1994	1 rockfall		2011	14 rockfalls	2×10^3
1995	2 landslides	6×10^3	2012	2 rockfalls	3×10^3
1997	1 rockfall		2013	13 rockfalls	30×10^3
1998	2 landslides 1 rockfall	4×10^3	2015	4 rockfalls	100

For each year, we have added up the volumes of the single landslides occurred

avalanche can be considered the largest movement recorded in the range during the past 65 years. Regarding their spatial distribution, 84% of the mass movements are located in the northern and coastal face of the range (Fig. 1). The first event considered was the Fornalutx earth slide; with a surface area of 40,000 m^2, and around 150,000 m^3 in volume, the landslide was triggered by continuous and persistent rainfall during the spring of 1954 (Mateos et al. 2008). Before 1954, the previous landslide recorded took place in 1924, and no rainfall data are available. Table 3 may wrongly suggest that the number of movements has increased since 2005; however, in earlier times only significant slope failures were reported, those reflected in the media. The landslide inventory is much more complete since 2005, when a thorough monitoring of the movements was started by the Geological Survey of Spain and the Road Maintenance Service of Mallorca. In this sense, we assume a lack of information in the inventory prior to 2005 that significantly weakens the results of the present research.

In relation to the meteorological factors which triggered the mass movements, rockfalls took place (Mateos et al. 2007, 2012): (1) after occurrences of intense rainfall >90 mm/24 h and (2) during rainy periods (accumulated rain >800 mm/3 months), regardless of whether the maximum daily rainfall was overly intense (around 30 mm). The main triggering factor for earth slides is a high, accumulated rainfall figure; the value of the rain intensity is less determining (Mateos et al. 2012). Referring to their temporal distribution, the available data show that most of the mass movements (98%) were triggered during the autumn and winter seasons.

4 Spectral analysis results

4.1 Power spectrum

The spatial distribution of rainfall is very irregular across the range, and the rainfall pattern varies considerably from one station to another, which means that rainfall data are heavily influenced by exceptional and local events as well as for the amplification of the rainfall signal across the mountain range due to the orographic impact (Mateos et al. 2012). In this sense, gauging station data series are more homogeneous and reliable than rainfall ones.

Figure 2 shows the power spectra obtained for (A) the Pollença rainfall station, (B) the Sant Miquel gauging station, and (C) the Font de s´Olla gauging station. As a general result, the annual cycle is the most significant in all data series, followed by the 6-month and NAO cycles. Additionally, the cycles related to the QBO, ENSO, Sun Spot and Hale Cycles are also represented, as well as others in relation to solar activity (42.7 yrs). A new finding in this analysis is the detection of the 17-year cycle in the Tramuntana Range related to lunar–solar activity and only described previously in speleothem studies (Currie et al. 1993). The analysis of the power spectra reveals that cycles with low frequency are better represented in the data series from gauging stations, and consequently, more cycles can be identified. Luque-Espinar et al. (2008) also reported this in previous research carried out in the Mediterranean region. The annual and 6-month cycles are well represented in all the series, for both rainfall and gauging stations. Nevertheless, the 6-month cycle is more statistically significant in the rainfall station dataset.

The analysis of data from the Pollença rainfall station (Fig. 2a) shows greater strength, and two statistically representative climate cycles were identified which are related to the ENSO and Hale cycles. The analysis of the Sant Miquel gauging station (Fig. 2b) reveals

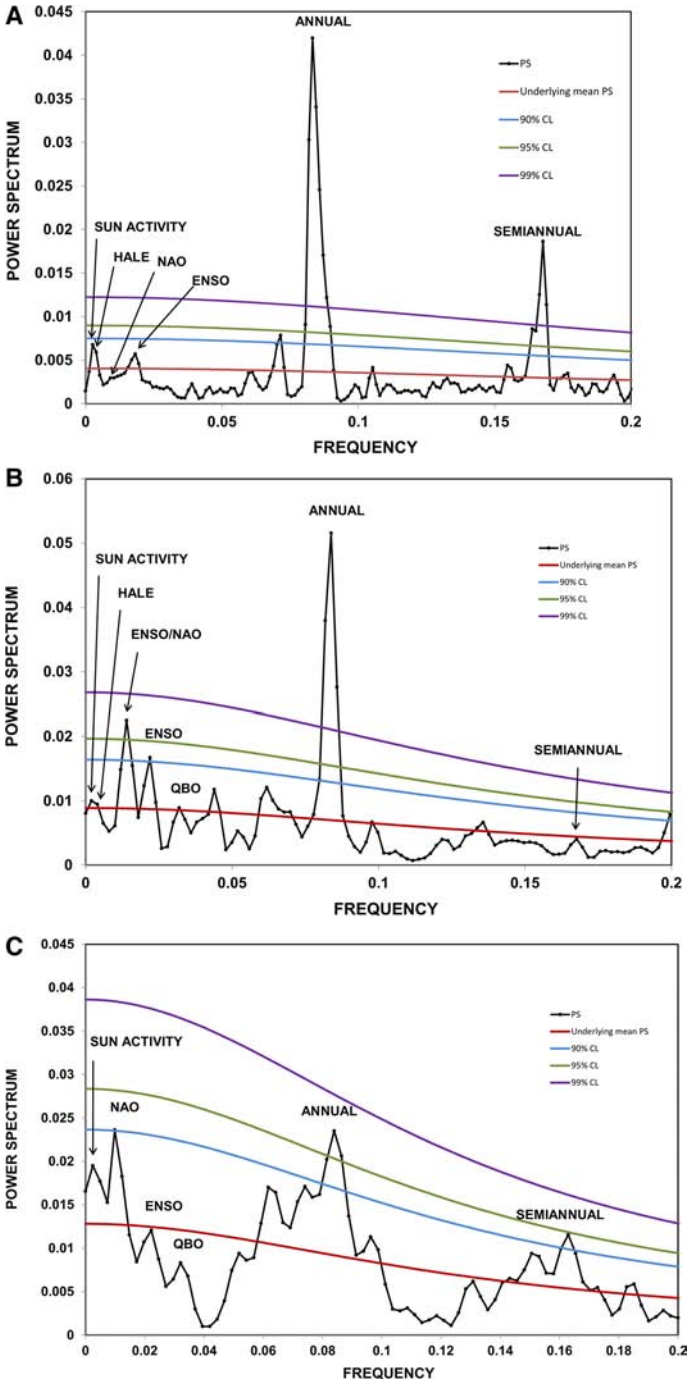

Fig. 2 Power spectra obtained for: **a** the Pollença rainfall station; **b** the Sant Miquel gauging station; and **c** the Font de s'Olla gauging station (see location in Fig. 1)

climate cycles related to the QBO, ENSO, NAO and Hale, with a higher statistical significance for the ENSO and NAO cycles, as well as the annual cycle. On the other hand, the Font de s´Olla gauging station located at the north-western edge of range shows that the most representative cycles are the ENSO and NAO (Fig. 2c). In this case, the NAO signal has the highest statistical significance (95% confidence).

5 Simulations

Taking into account the most significant cycles obtained for each rainfall/gauging station, around 174 simulations have been performed. Due to their higher spectral value, cycles with high frequency (annual and semi-annual) reproduce quite well the real rainfall data. Figure 3 shows this, where a simulation carried out in the Pollença rainfall station, representing the annual and semi-annual cycles, provides a good fit to monthly rainfall. Nevertheless, the strength of the annual and semi-annual cycles can partially mask the importance of intermediate frequency cycles (between 3 and 11 years), which are usually related to heavy rainfall episodes. Based on this, annual and semi-annual cycles were not used.

The simulation conducted in this work is a sine wave (cosine function) where amplitude and frequency values are obtained from the results of the spectral analysis, considering a monthly temporal unit. When different climatic cycles (sinusoidal functions) are simulated, values obtained in each simulation—performed individually—are simply added. Additionally, the moving annual average has been incorporated in order to see the annual behaviour of the time series and the accuracy of the simulations. Taking into account the number of climate cycles previously detected (7 in the whole Tramuntana Range), 25 simulations for each time series have been performed: first individually and later combined.

At a second stage, a superpositioning of the landslide events over the simulated curves was carried out to determine the matching (or mismatching) between rainy periods and

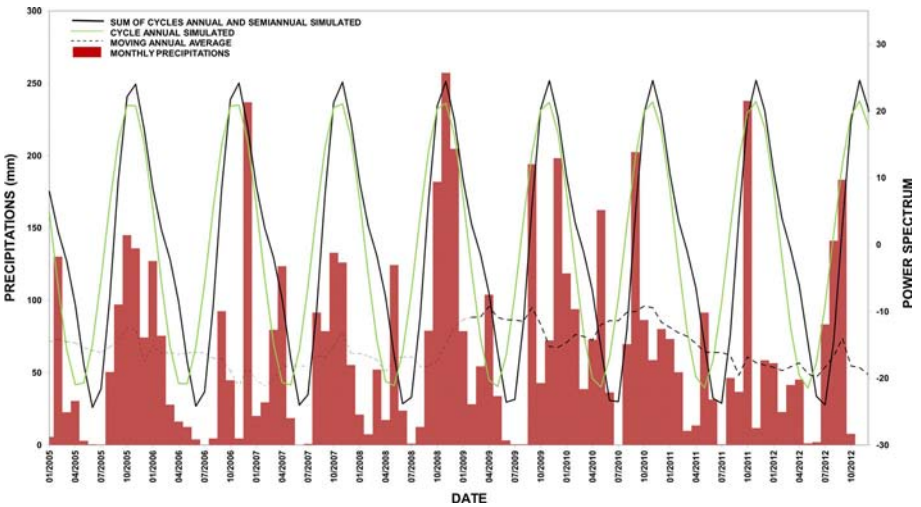

Fig. 3 Simulation carried out in the Pollença rainfall station for the period spanning from 2005 to 2012

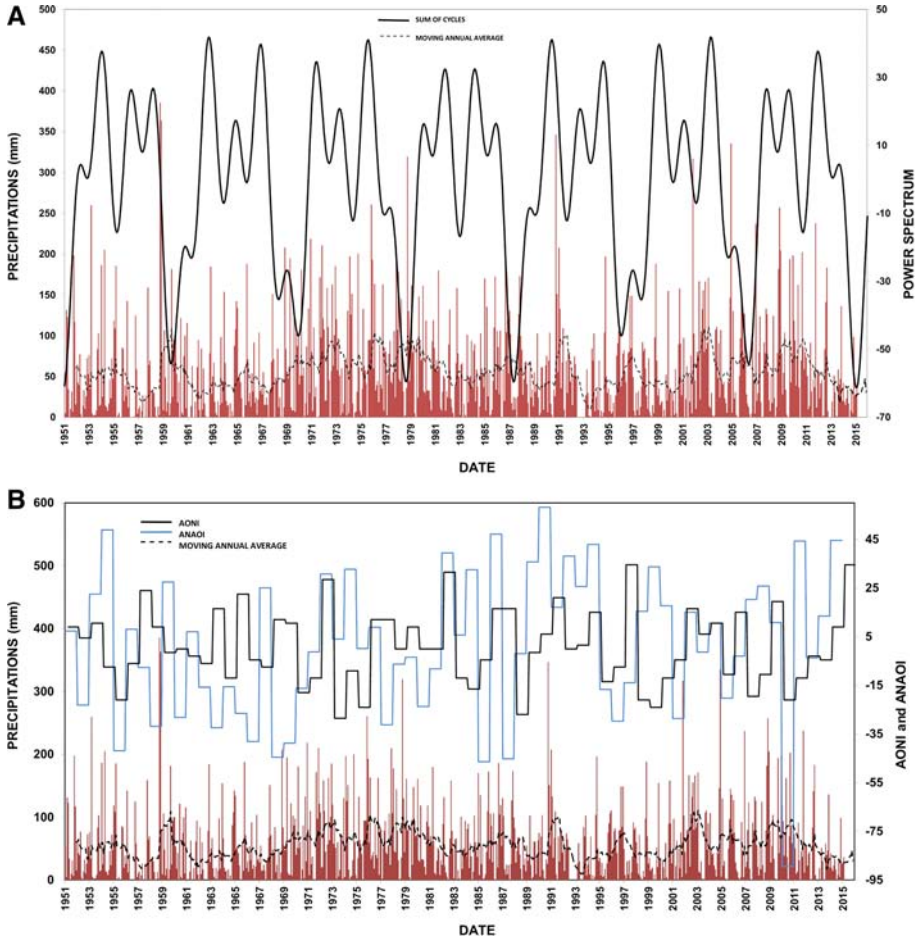

Fig. 4 **a** Simulation results for the Pollença rainfall station considering the sum of the 3.8 + 6.1 + 28-year cycles. **b** Correlation between rainfall data recorded in the Pollença rainfall station and both the Annual Oceanic Niño Index (AONI) (NOAA 2016) and the Annual North Atlantic Oscillation Index (ANAOI) (NCARS 2016)

landslide occurrence, that is: if landslides are/not are related to rainy peaks by means of visual observations, with the subsequent objective of predicting future hazardous situations. Based on the outputs obtained, the best simulation from the 174 performed has been selected; that is where the simulation fits with the experimental data (rainfall/flows) best.

After numerous attempts, the three simulations corresponding to: the Pollença rainfall station (Fig. 4), the Sant Miquel gauging station (Fig. 5) and the Gross Palma gauging station, were selected (Fig. 6). They represent the variability in the data source and their spatial distribution. In the three cases, the most significant climate cycles identified have been considered. On the other hand, the simulations developed for Palma rainfall station, Escorca rainfall station and Font de S´Olla gauging station present a high level of noise, and a low confidence is obtained with the simulations. We suspect serious measurement errors in the datasets.

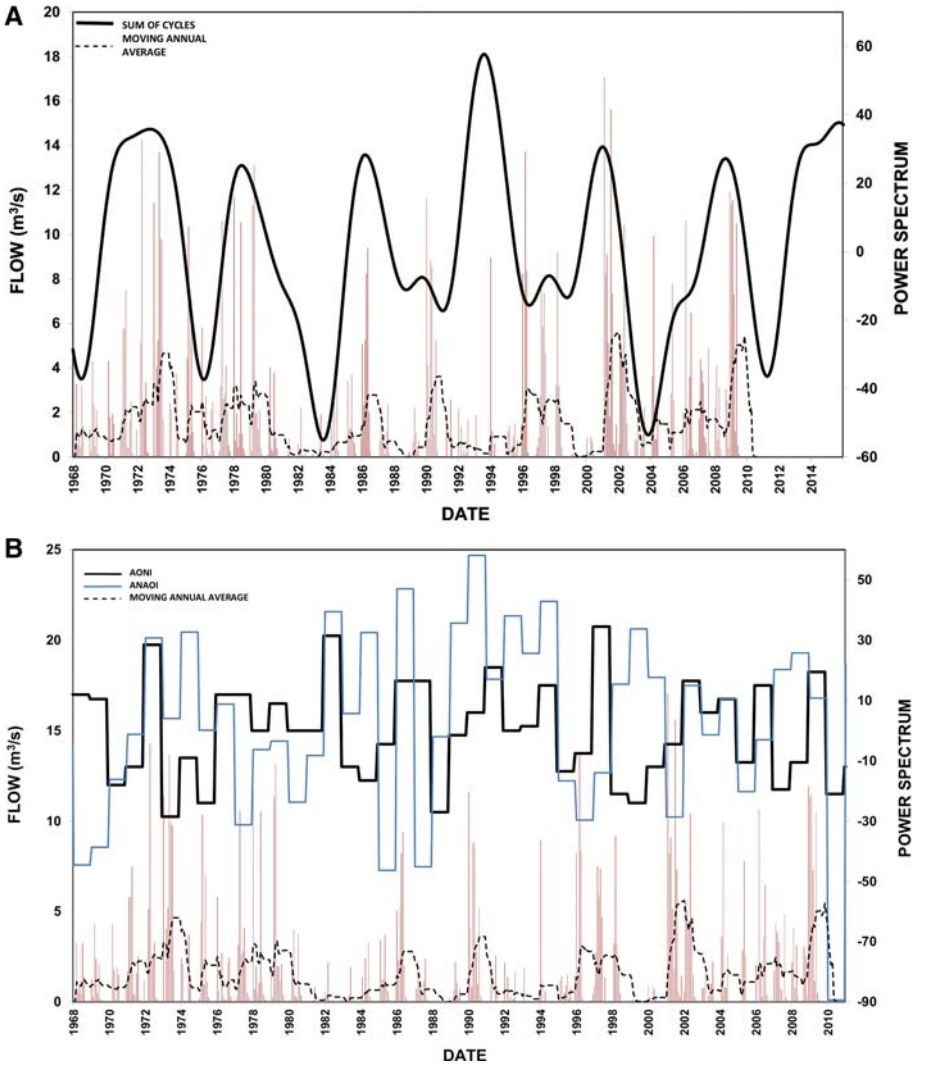

Fig. 5 **a** Simulation results for the Sant Miquel gauging station considering the sum of the 3.8 + 6.1 + 21-year cycles. **b** Correlation between flow data and both the Annual Oceanic Niño Index (AONI) (NOAA 2016) and the Annual North Atlantic Oscillation Index (ANAOI) (NCARS 2016)

Figure 4a shows the results for the Pollença rainfall station. The simulated curve has been developed considering the sum of the ENSO + NAO + 28-year cycles, as they are the most significant cycles in the power spectrum (Fig. 2a). Rainfall values are superimposed onto the simulated curve (Fig. 4a) to determine the accuracy of the simulation. Additionally, rainfall data have also been correlated with the Annual Oceanic Niño Index (AONI) (NOAA 2016) and the Annual North Atlantic Oscillation Index (ANAOI) (NCARS 2016) in order to determine the most influential cycle in the rainiest events (Fig. 4b). The same procedure has been carried out for the Sant Miguel gauging station (Fig. 5a, b) and for Gross Palma gauging station (Fig. 6a, b). In the case of Gross Palma,

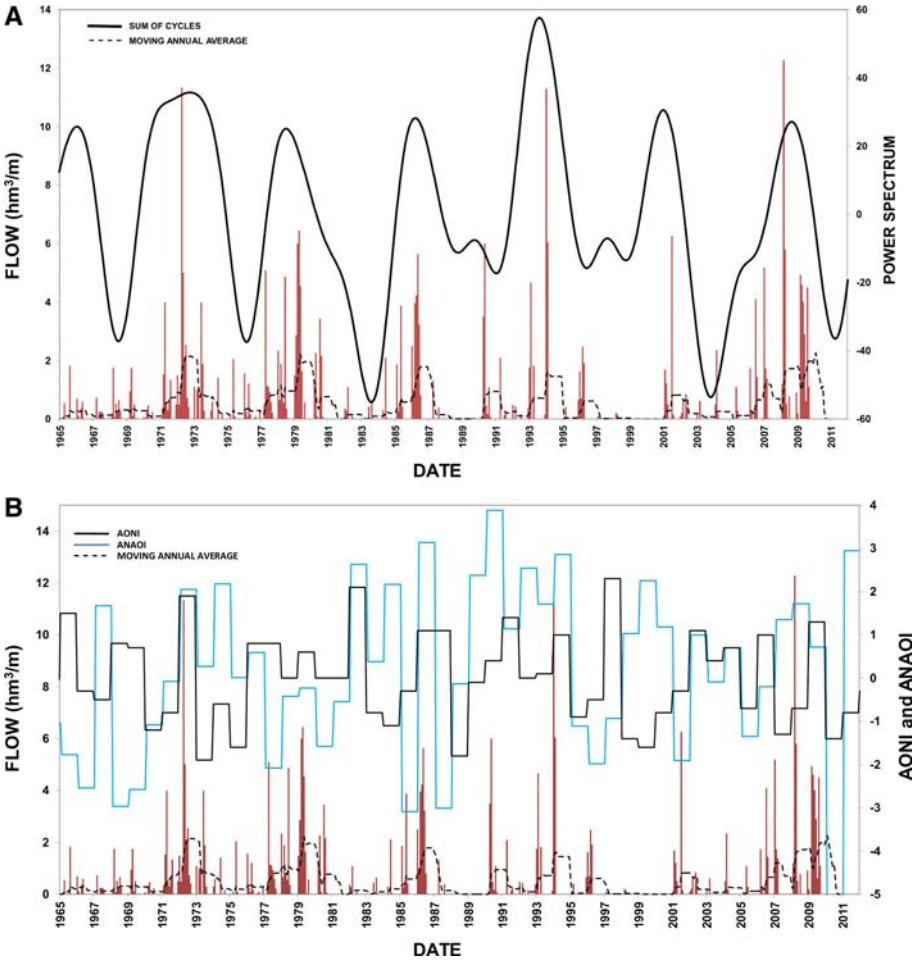

Fig. 6 **a** Simulation results for the Gross Palma gauging station considering the sum of the 3.8 + 7.1 + 21-year cycles. **b** Correlation between flow data and both the Annual Oceanic Niño Index (AONI) (NOAA 2016) and the Annual North Atlantic Oscillation Index (ANAOI) (NCARS 2016)

the simulation has been performed considering the ENSO + NAO + 21-year cycles (Fig. 6a).

In the present work, the statistical coefficients of correlation between the rainfall/flow series and the AONI and ANAOI indexes are low (around 0.2) and specifically for the rainfall series. The best results (more than 0.4) are obtained when flow data are used, and they are correlated with the sum of both indexes (ANAOI + AONI). Recent studies (Qu et al. 2012; Trigo et al. 2004) tried to correlate numerous parameters such as surface sea temperature, ice cover, precipitation, river flow and water resources with the ANAOI index, and they obtained a large variety of values in the correlation coefficients. In fact, the association between the NAO circulation mode and the surface climate of the European continent has recently been shown to be non-stationary, i.e. the strength of the correlation between the NAO index and local (or regional) climate variables has changed over time (Goodess and Jones 2002; Rodó et al. 1997; Trigo et al. 2004).

The NAO and ENSO cycles show the best correlation, and specifically the NAO cycle. This is clearly observed in Fig. 5a, b, where the highest flows recorded have the same periodicity (cadence) than the NAO and ENSO cycles (Fig. 2). In all the cases, a good correlation between episodes of high rainfall and high values of ANAOI can be observed and, to a lesser extent, with AONI (Figs. 4b, 5b, 6b). Additionally, rainy years such as 1972, 1979, 1986, 2008, 2009 and 2010 are related to the coincidence of high values of both the NAO and the ENSO.

6 Simulation versus landslide occurrence

The Pollença rainfall station and the Sant Miquel gauging station simulations are going to be considered in the correlation stage with the landslide inventory. The selection criteria are: (1) Pollença is the most representative and reliable rainfall station in the range; (2) Sant Miquel gauging station has the longest continuous series and data are not human influenced; and (3) Gross Palma gauging station is located near an urban area with probable anthropogenic influences in the dataset. Based on this, the simulations obtained in the previous stage for Pollença and Sant Miquel are used to develop two temporal correlations:

6.1 Period 2005–2015

A correlation was carried out between both simulations and the landslide events recorded during the period 2005–2015, when the landslide inventory is much more complete (Fig. 7). We have considered 157 events (20 landslides and 137 rockfalls) perfectly dating during this period and monthly grouped. Figure 7a shows the correlation obtained for the Pollença rainfall station and Fig. 7b those corresponding to Sant Miquel gauging station. Both figures clearly show a wetter period between 2006 and 2011 where most of the landslides took place, which coincides with high values of AONI and specifically of ANAOI (Fig. 4b). This correlation is even better between November 2008 and January 2009, when a total of 640,000 m^3 of rock material were mobilised (45% of the total volume recorded in the whole study series). The Son Cocó rock avalanche was triggered within this period (Dec 2008) when maximum rainy and flow peaks were recorded and within high values of both simulation curves. Comparing both figures, a better correlation is obtained for Sant Miquel.

An interesting event was January 2006 when 22 rockfalls were recorded (all of them with very low magnitudes) but no landslides. We have confirmed that these rockfalls took place in a very limited area and concentrated in the last 4 days of January 2006. The event coincided with low values of AONI and ANAOI and rockfalls could be related to a local and intense rainfall event.

6.2 Period 1968–2010

Based on the previous analysis, the Sant Miquel gauging station simulation (Fig. 5) has been selected for a general correlation, considering all the mass movements inventoried (Table 3) for the period with flow data available (1968–2010). Figure 8 shows this correlation where the hazardous events have been classified based on the number of landslides recorded. Most of the high simulated values coincide with landslide events, and they are

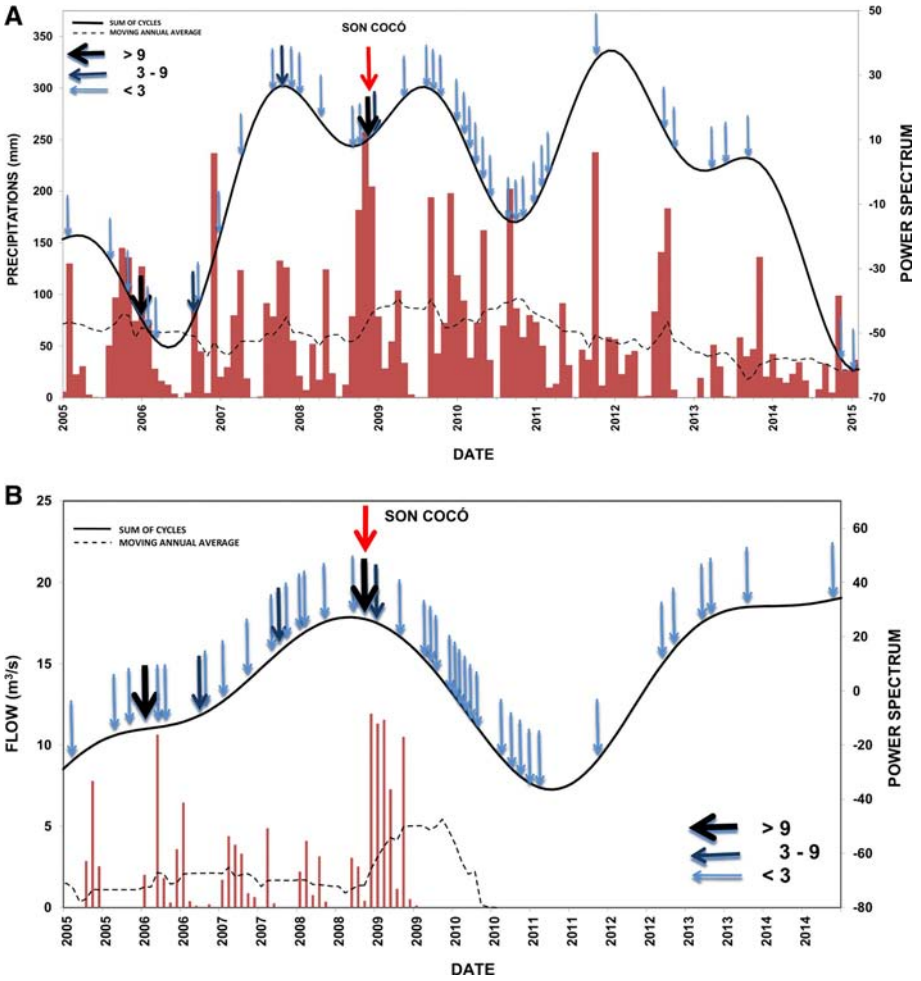

Fig. 7 Correlation between landslide events and the simulations carried out (the *thickness of the arrows* indicates the number of landslide events): **a** Pollença rainfall station (2005–2014); **b** Sant Miquel gauging station (2005–2009)

related to high values of ANAOI. The hazardous period 2008–2010 took place when the NAO and ENSO cycles coincided and after a drought period in the region. Since 2010, mass movement (rockfalls) events still occur but they are narrowing in number and magnitude.

For both periods, if we only take into consideration earth slides, most of them (65%) took place in a temporal window of 8 months after the maximum in the simulated peaks, that is: after a high accumulated rainfall figure. Nevertheless, rockfalls are distributed more irregularly over time, and they can be related to punctual intense rainy events as well as to freeze–thaw cycles prior to the failure, as the work done by Mateos et al. (2012) refers.

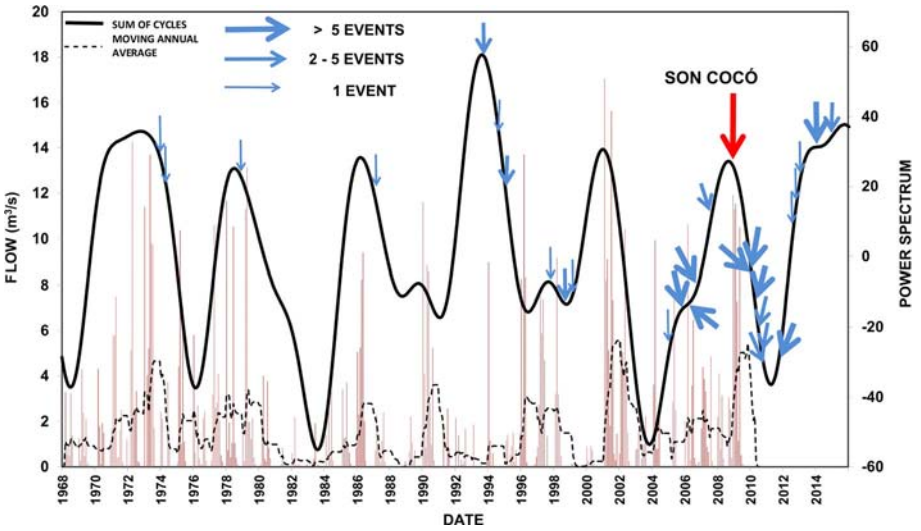

Fig. 8 Correlation between the landslide inventory (Table 3) and the simulation carried out for Sant Miquel gauging station, and for the period spanning 1968–2010

7 Discussion and conclusions

The combination of rainfall data with flow rates from natural springs and/or stream/rivers can generate very reliable climate simulations. The incorporation of gauging station data time series as climate proxies considerably improves the results, as the data are inherently filtered and irrelevant signals are deleted in the simulation. The present work confirms this, specifically when the data derived from natural springs, with scarce human intervention, is used. Nevertheless, in the present case some data series from rainfall and gauging stations have been considered unreliable; in this sense, power spectrum analysis has proven to be an effective tool to identify this weakness in the starting data. Based on this, Font de S´Olla gauging station as well as Escorca and Palma rainfall stations were rejected in the simulation stage.

Climate signals recorded previously in the Mediterranean region have been identified in the present research: the ENSO, QBO, NAO, Sun Spot and Hale Cycles as well as others related to solar activity. They confirm the climatic complexity of the Tramuntana Range area, located on the western Mediterranean. Spectrum analysis reveals that the annual cycle is the most significant in the region, followed by the 6-month and NAO cycles. A new finding in this analysis is the detection of the 17-year cycle in the Tramuntana Range related to solar/lunar activity, only described previously in speleothem studies.

Cycles with high frequency, annual and semi-annual, because of their higher spectral value, can partially mask the importance of intermediate frequency cycles (between 3 and 11 years), which are related to intense rainfall periods. Based on this, annual and semi-annual cycles have not been incorporated into the simulations.

Simulations have been developed taking into consideration the most reliable data series from: Sant Miquel gauging station, Pollença rainfall station and Gross Palma gauging station. In general, rainfall and flow values match the simulated curves well. The NAO and ENSO show the best correlation and specifically the NAO cycle, where a good correlation between episodes of high rainfall and high values of ANAOI can be observed. The impact

of the North Atlantic Oscillation (NAO) on winter precipitation was already documented in southern Iberia with regard to river flow regimes, with large disparities between wet and dry years (Trigo et al. 2004; Luque-Espinar et al. 2008). This result may reinforce the idea that hydrological hazards are largely modulated by the NAO in the Spanish Mediterranean region. Additionally, some rainy episodes are related to the coincidence of high values of both the ANAOI and AONI Indices. In these cases, the sum of both climatic indexes reproduces more accurately the experimental values of the simulated hydrological series. The best results are obtained when working with the flow data, and specifically at the Sant Miguel gauging station.

The complexity of the relationship between mass movements and climatic conditions makes it difficult to define "universal laws". Climate is never the sole cause (Flageollet et al. 1999; Dikau and Schrott 1999). Nevertheless, some authors consider that modifications in mass movement frequency may be interpreted as changes in the hydrological conditions of slopes, which are directly controlled by climate. In the present work, regarding the correlation between landslide events and simulations, hazardous events are in general associated with the periods of highest rainfall/flow values in the simulated curves. As a general observation, we can determine that landslide events are mainly related to the NAO cycle. The correlation for the past decade (since 2005), when a detailed landslide inventory is available, also reveals a coincidence between landslide events and climate cycles overlapping, and specifically NAO and ENSO cycles. That is the case of the period 2008–2010, when numerous mass movements took place, and when the largest movement, the Son Cocó rock avalanche, was recorded. Nevertheless, we have identified a hazardous event in January 2006 where numerous small rockfalls took place, concentrated in space and time. This event coincided with low values of AONI and ANAOI. In this sense, the impact of orographic rainfall could be significant, but it has not been contemplated in the study.

To show the potential of this methodology to predict future hazardous events in the Tramuntana range for the coming years, we have represented the most significant landslide events, with magnitudes over 1000 m^3, over the simulated curve for the Sant Miquel gauging station, that starts in 1951 and have continuity into the future until 2049 (Fig. 9). Simulation shows a potential rainy period which could begin in 2017 and with maximum values around 2021. Similar conditions to those related to the 2008–2010 event could take place again during that period. This prediction has partially been confirmed as the 2017 winter in Majorca registered heavy rainfall and snowfall in the Tramuntana range. During the months of January and February 2017, seven rockfalls occurred in different areas of the mountain range and they seriously affected the road network of the range.

Finally, we can conclude that spectral analysis, when applied to hydrological long-term series, can identify the statistical significance of natural climate cycles in a region with accuracy. Taking into account that landslide hazards are closely related to unusual rainfall events and they are largely modulated by the natural climate cycles and their overlap, the methodology presented in this work can contribute to regional landslide temporal prediction in order to design short-/medium-term mitigation strategies. The approach here presented can be applied in other regions where a long series of rainfall, foronomic and piezometric data are available and a detailed landslide inventory exits. New test sites with a record of at least 20 years of hydrological and landslide data can contribute to carry out a more robust analysis.

This methodology could be considerably improved if we can introduce local meteorological factors, which also contribute to the generation of landslides. Additionally, new mathematical tools have to be developed to carry out a quantitative evaluation of the

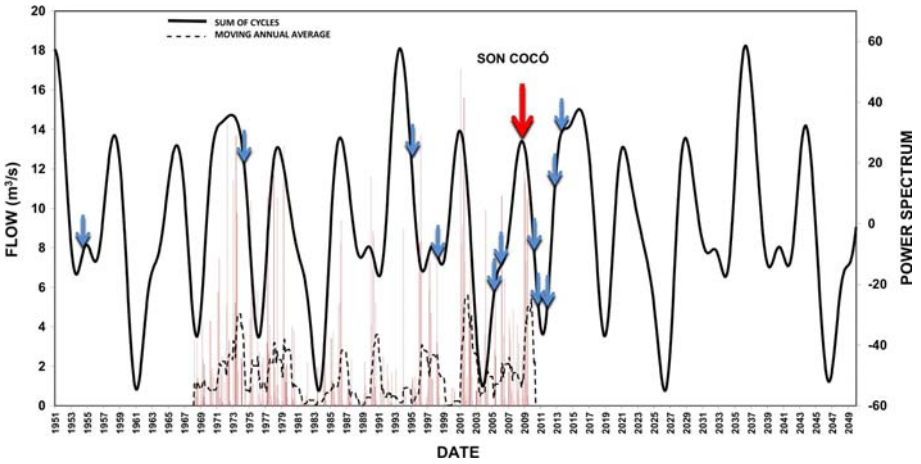

Fig. 9 Correlation between the most significant landslide events (over 1000 m^3 in volume) and the simulation developed for the Sant Miquel gauging station which has been extended to 2049. Simulation shows a potential, close in time rainy period which could begin in 2017 and with maximum values around 2021

relationship between climate cycles and landslide occurrence. New test sites in the Mediterranean region, with long time series of data, could improve the methodology here presented and support the results obtained.

Acknowledgements The research leading to these results has received funding from the European Union Seventh Framework Programme (FP7/2007-2013) under Grant Agreement No. 312384. LAMPRE Project. Additionally, this work was partially supported by the Ministerio de Economía y Competitividad of Spain, KARSCLIMA Project CGL2015-71510-R. Special thanks to the Regional Water Agency of the Balearic Islands and especially to their technical team for providing data from gauging stations.

References

Blackman RB, Tukey JW (1958) The measurement of power spectra from the point of view of communication engineering. Bell Syst Tech J 37:185–282

Bras RL, Rodríguez-Iturbe I (1985) Random functions and hydrology. Addison-Wesley, Reading, p 559

Burg JP (1972) The relation between maximum entropy spectra and maximum likelihood spectra. Geophysics 37:375–376

Capparelli G, Versace P (2011) FLaIR and SUSHI: two mathematical models for early warning of landslides induced by rainfall. Landslides 8:67

Coe JA, Godt JW (2012) Review of approaches for assessing the impact of climate change on landslide hazards. In: Eberhardt E, Froese C, Turner AK, Leroueil S (eds) Landslides and engineered slopes, protecting society through improved understanding: proceedings 11th international and 2nd North American symposium on landslides and engineered slopes, Banff, Canada 1. Taylor & Francis, London, pp 371–377

Corominas J (2006) El clima y sus consecuencias sobre la actividad de los movimientos de ladera en España. Cuaternario y Geomorfología 20:89–113

Crozier MJ (2010) Deciphering the effect of climate change on landslide activity: a review. Geomorphology 124:260–267

Currie RG, Wyatt T, O'Brien DP (1993) Deterministic signals in European fish catches, wine harvest and sea level, and further experiments. Int J Climatol 13:665–687

Dikau R, Schrott L (1999) The temporal stability and activity of landslide in Europe with respect to climatic change (TESLEC): main objectives and results. Geomorphology 30:1–12

Flageollet JC, Maquaire O, Martin B, Weber D (1999) Landslides and climatic conditions in the Barcelonnette and Vars basins (Southern French Alps, France). Geomorphology 30:65–78
Fleming SW, Quilty E (2006) Aquifer responses to El Niño-Sothern Oscillation, Southwest British Columbia. Ground Water 44:595–599
Gariano SL, Guzzetti F (2016) Landslides in a changing climate. Earth Sci Rev 162:227–252
Gelabert B (2002) Las Fonts Ufanes (Mallorca): funcionamiento hidráulico de una surgencia kárstica. Boletín de la Sociedad Española de Espeleología y Ciencias del Karst 3:46–55
Goodess CM, Jones PD (2002) Links between circulation and changes in the characteristics of Iberian rainfall. Int J Clim 22:1593–1615
Guzzetti F, Peruccacci S, Rossi M, Colin PS (2008) The rainfall intensity- duration control of shallow landslides and debris flows: an update. Landslide 5:3–17
Hoyt DV, Schatten KH (1997) The role of the Sun in climate change. Oxford University Press, Oxford, p 279
Huang J, Ju NP, Liao YJ, Liu DD (2015) Determination of rainfall thresholds for shallow landslides by a probabilistic and empirical method. Nat Hazards Earth Syst Sci 15:2715–2723
Hurrell JW (1995) Decadal trends in the North Atlantic Oscillation, regional temperatures and precipitation. Nature 269:676–679
Jenkins GM, Watts DG (1968) Spectral analysis and its applications. Holden-Day, San Francisco, p 525
Karagiannidis AF, Bloutsos AA, Maheras SachsamanoglouC (2007) Some statistical characteristics of precipitation in Europe. Theor Appl Climatol 91:193–204
Knippertz P (2003) Tropical-extratropical interactions causing precipitation in Northwest Africa: statistical analysis and seasonal variations. Mon Weather Rev 131:3069–3076
Labitzke K, van Loon H (1990) Associations between the 11-year solar cycle, the Quasi-Biennial Oscillation and the atmosphere: a summary of recent work. Philos Trans R Soc Lond 330:577–589
Lamb HH (1977) Climate: past, present and future climatic history and the future, vol 2. Methuen, London
Luque-Espinar JA, Chica-Olmo M, Pardo-Igúzquiza E, García-Soldado MJ (2008) Influence of climatological cycles on hydraulic heads across a Spanish aquifer. J Hydrol 354:33–52
Luque-Espinar JA, Chica-Olmo M, Pardo-Igúzquiza E, Rodríguez Galiano V (2013) Simulación de niveles piezométricos basada en los ciclos climáticos. In: Uría AF (ed) Proceedings X Simposio Nacional de Hidrogeología, Granada, vol 1, pp 815–820
Mateos RM (2002) Slope movements in the Majorca Island (Spain). In: McInnes RG, Jakeways J (eds) Hazard analysis. Instability, planning and management. Seeking sustainable solutions to ground movements problems. Thomas Telford, London, pp 339–346
Mateos RM (2006) Los movimientos de ladera en la Serra de Tramuntana (Mallorca). Caracterización geomecánica y análisis de peligrosidad. PhD. Servicio de Publicaciones de la Universidad Complutense de Madrid. Madrid, p 299
Mateos RM, González C (2009) Los Caminos del Agua en las Islas Baleares. Acuíferos y Manantiales. Published by: Instituto Geológico y Minero de España & Conselleria de Medi Ambient del Govern de les Illes Balears, p 315
Mateos RM, Azañón JM, Morales R, López-Chicano JM (2007) Regional prediction of landslides in the Tramuntana Range (Majorca) using probability analysis of intense rainfall. Zeitschrift für Geomorphology, Nº 51, 3:287–306
Mateos RM, Bermejo M, Hijazo T, Rodríguez-Franco JA, Ferrer M, González de Vallejo LI, Garcia I (2008) Los deslizamientos de la ladera de la margen izquierda del torrente de Fornalutx (Mallorca). Boletín Geológico y Minero 119:443–458
Mateos RM, García-Moreno I, Azañón JM, Tsige M (2010) La avalancha de rocas de Son Cocó (Alaró, Mallorca). Descripción y análisis del movimiento. Boletín Geológico y Minero 121(2):153–168
Mateos RM, García-Moreno I, Azañón JM (2012) Freeze-thaw cycles and rainfall as triggering factors of mass movements in a warm Mediterranean region: the case of the Tramuntana Range (Majorca, Spain). Landslides 9:417–432
Mateos RM, García- Moreno I, Herrera G, Mulas J (2013) Recent mass movements in the Tramuntana Range (Mallorca, Spain). In: Margottini C, Canuti P, Sassa K (eds) Landslide science and practice, volume 4. Global Environmental Change, pp 27–37
Mateos RM, Garcia-Moreno I, Reichenbach P, Herrera G, Sarro R, Rius J, Aguiló R (2015) Calibration and validation of rockfall modelling at regional scale: application along a roadway in Mallorca (Spain) and organization of its management. Landslides. doi:10.1007/s10346-015-0602-5
Mathew J, Babu DG, Kundu S, Vinod Kumar K, Pant CC (2014) Integrating intensity-duration-based rainfall threshold and antecedent rainfall-based probability estimate towards generating early warning for rainfall-induced landslides in parts of the Garhwal Himalaya, India. Landslides 11(4):575–588

Muñoz-Díaz D, Rodrigo FS (2005) Influence of El Nino-Sothern Oscillation on the probability of dry and wet seasons in Spain. Clim Res 30:1–12

NCARS, National Center for Atmospheric Research Staff (2016) The climate data guide: Hurrell North Atlantic Oscillation (NAO) Index (PC-based). Retrieved from http://climatedataguide.ucar.edu/climate-data/hurrell-north-atlantic-oscillation-nao-index-pc-based. See more at: http://climatedataguide.ucar.edu/climate-data/hurrell-north-atlantic-oscillation-nao-index-pc-based#sthash.F0WaOel7.zFyy9CyX.dpuf. Accessed 30 Mar 2016

NOAA, National Oceanic and Atmospheric Administration (2016) Annual Oceanic Niño Index. http://www.cpc.ncep.noaa.gov/products/analysis_monitoring/ensostuff/detrend.nino34.ascii.txt. Accessed 9 March 2016

Papoulis A (1984) Probability, random variables and stochastic processes. McGraw-Hill, Singapore

Pardo-Igúzquiza E, Rodriguez-Tovar FJ (2004) POWGRAF2: a computer program for graphical spectral analysis. Comput Geosci 30(5):533–542

Pardo-Igúzquiza E, Rodríguez-Tovar FJ (2012) Spectral and cross-spectral analysis of uneven time series with the smoothed Lomb–Scargle periodogram and Monte Carlo evaluation of statistical significance. Comput Geosci 49:207–216

Pardo-Igúzquiza E, Chica-Olmo M, Rodríguez-Tovar FJ (1994) CYSTRATI: a computer program for spectral analysis of stratigrafic successions. Comput Geosci 20:511–584

Piciullo L, Gariano SL, Melillo M, Brunetti MT, Peruccacci S, Guzzetti F, Calvello M (2016) Definition and performance of a threshold-based regional early warning model for rainfall-induced landslides. Landslides. doi:10.1007/s10346-016-0750-2

Pozo-Vázquez D, Esteban-Parra MJ, Rodrigo FS, Castro-Díez Y (2000) An analysis of the variability of the North Atlantic Oscillation in the time and the frequency domains. Int J Climatol 20:1675–1692

Qu B, Gabric AJ, Zhu J, Lin D, Qian F, Zhao M (2012) Correlation between sea surface temperature and wind speed in Greenland Sea and their relationships with NAO variability. Water Sci Eng 5(3):304–315

Rodó X, Baert E, Comin FA (1997) Variations in seasonal rainfall in Southern Europe during the present century: relationships with the North Atlantic Oscillation and the El Niño-Southern Oscillation. Clim Dyn 13:275–284

Saaroni H, Toseti A, Trigo IF, Vicente-Serrano SM, Yiou P, Ziv B (2012) Large-scale atmospheric circulation driving extreme climate events in the Mediterranean and its related impacts. In: Lionello P (ed) The climate of the Mediterranean region. Elsevier, USA, pp 347–403

Staley DM, Kean JW, Cannon SH, Schmidt KM, Laber JL (2013) Objective definition of rainfall intensity-duration thresholds for the initiation of post-fire debris flows in southern California. Landslides 10:547–562

Stuiver M, Braziunas TF (1989) Atmospheric 14C and century-scale solar oscillations. Nature 338:405–408

Terlien MTJ (1998) The determination of statistical and deterministic hydrological landslide-triggering threshold. Environ Geol 35:125–130

Thomson DJ (1982) Spectrum estimation and harmonic analysis. Proc IEEE 70(9):1055–1096

Tramblay Y, El Adlouni S, Servat E (2013) Trends and variability in extreme precipitation indices over Maghreb countries. Nat Hazards Earth Syst Sci 13:3235–3248

Trigo RM, Pozo- Vázquez D, Osborn TJ, Castro- Díez Y, Gámiz-Fortis S, Esteban-Parra J (2004) North Atlantic Oscillation influence on precipitation, river flow and water resources in the Iberian Peninsula. Int J Climatol 24:925–944

Wieczoreck GF (1996) Landslide triggering mechanisms. In: Turner AK, Schuster RL (eds) Landslides: investigation and mitigation. Transportation Research Board, National Research Council, Special report, Washington, DC, pp 76–90

Williams GE (1981) Sunspot periods in the late Precambrian glacial climate and solar-planetary relations. Nature 291:624–628

Xoplaki E, Trigo RM, García-Herrera R, Barriopedro D, D'Andrea F, Fischer EM, Gimeno L, Gouveia C, Hernández E, Kuglitsch FG, Mariotti A, Nieto R, Pinto JG, Pozo-Vázquez D, Saaroni H, Toreti A, Trigo IF, Vicente-Serrano SM, Yiou P, Ziv B (2012) Large-scale atmospheric circulation driving extreme climate events in the Mediterranean and its related impacts. In: Lionello P (ed) The climate of the Mediterranean region. Elsevier, USA, pp 347–403

Yevjevich V (1972) Stochastic processes in hydrology. Water Resources Publications, Fort Collins, p 276